Preparation and Properties of Asphalt Binders Modified by THFS Extracted From Direct Coal Liquefaction Residue

Jie Ji [1,2,*], Hui Yao [3,*] , Wenhua Zheng [1], Zhi Suo [1], Yuefeng Shi [4], Ying Xu [1], Hao Wu [1,2] and Zhanping You [3]

1   School of Civil Engineering and Transportation, Beijing University of Civil Engineering and Architecture, Beijing 100044, China; wenhuazheng@126.com (W.Z.); suozhi@bucea.edu.cn (Z.S.); xuying@bucea.edu.cn (Y.X.); wuhao710521732@163.com (H.W.)
2   Beijing Advanced Innovation Center for Future Urban Design, Beijing 100044, China
3   Department of Civil and Environmental Engineering, Michigan Technological University, 1400 Townsend Drive, Houghton, MI 49931, USA; zyou@mtu.edu
4   China Academy of Railway Sciences, Railway Engineering Research Institute, Beijing 100081, China; boyshiyuefeng@126.com
*   Correspondence: jijie@bucea.edu.cn (J.J.); huiyao@mtu.edu (H.Y.)

Abstract: This paper aims to study the preparation and viscoelastic properties of asphalt binder modified by tetrahydrofuran soluble fraction (THFS) extracted from direct coal liquefaction residue. The modified asphalt binders, which blended with SK-90 (control asphalt binder) and 4%, 6%, 8% and 10% THFS (by weight of SK-90), were fabricated. The preparation process for asphalt binder was optimized in terms of the orthogonal array test strategy and gray correlation analysis results. The properties of asphalt binder were measured by applying Penetration performance grade and Superpave performance grade specifications. In addition, the temperature step and frequency sweep test in Dynamic Shear Rheometer were conducted to predict the rheological behavior, temperature and frequency susceptibility of asphalt binder. The test results suggested the optimal preparation process, such as 150 °C shearing temperature, 45 min shearing time and 4000 rpm shearing rate. Subsequently, the addition of THFS was beneficial in increasing the high-temperature properties but decreased the low-temperature properties and resistance to fatigue. The content analysis of THFS showed the percentage of 4~6% achieved a balance in the high-and-low temperature properties of asphalt binder. The asphalt binder with higher THFS content exhibited higher resistance to rutting and less sensitivity to frequency and temperature.

Keywords: direct coal liquefaction residue; tetrahydrofuran soluble fraction; THFS; preparation process; viscoelastic properties; temperature susceptibility; frequency susceptibility

1. Introduction

In 1900, Friedrich Bergius first discovered the coal to liquid fuels (CTL) technique and since then, this technology has evolved rapidly, especially in China [1,2]. At present, China has built lots of projects to utilize the CTL technology, such as SHENHUA project, YUNNAN project, etc. Actually, CTL is a refinery process to convert coal into liquid hydrocarbons: liquid fuels and petrochemicals, such as petrol, diesel, and liquefied petroleum gas etc. Therefore, CTL is commonly called coal liquefaction. Coal liquefaction technologies generally fall into two categories: direct coal liquefaction (DCL) and indirect coal liquefaction (ICL) processes [3,4]. DCL processes convert coal into liquids directly, without the intermediate step of gasification, by breaking down its organic structure with the application of

solvents or catalysts in a high pressure and temperature environment and is applied widely in China. However, the direct coal liquefaction residue (DCLR) is the main by-product generated in the DCL process, which accounts for 30% by weight of raw coal. Currently, both in China and overseas, DCLR is mainly used as a feedstock for gasification or combustion, which will not only cause serious environmental pollution but also reduce its economic value and lead to a waste of valuable resources. If DCLR were applied for asphalt pavement construction, it would be economical and beneficial, and can potentially reduce the environmental pollution in China [5]. How to utilize DCLR in a friendly and economical way is always a big issue [6,7].

Recently, some asphalt modifiers (e.g., styrene-butadiene-styrene (SBS), rubber, acids) are commonly used in the pavement construction because of their excellent performances. Behnood, Kök et al. evaluated rheological, elastic and low-temperature properties of SBS, ground tire rubber (GTR) and polyphosphoric acid (PPA) modified asphalt binder respectively. The results showed that all of the modifiers could improve the high-temperature properties and had not significant effects on the low-temperature continuous grade [8–10]. Being that DCLR contains 30~50% heavy oil and asphaltene materials and is a very valuable resource material, it has the potential to be developed into asphalt modifier [11,12]. Ji et al. tested the properties and microstructure of SK-90, which is a commercial brand asphalt binder, blended with different DCLR contents using various test methods, such as Superpave performance grade specification, Penetration performance grade specification, infrared spectrometer, and gel permeation chromatography. The test results indicated that the high-temperature properties of DCLR modified asphalt binder improved, but the low-temperature properties and fatigue cracking resistance of asphalt binder declined [13]. Zhang et al. measured the surface energies of three DCLR modified asphalt binders, the test results showed that the water sensitivities of the three DCLR modified asphalt binders combined with aggregates were better than those of the base asphalt binder [14].

However, although DCLR can improve the high-temperature properties and water sensitivity of asphalt binder, the low-temperature properties and fatigue cracking resistance declined because DCLR contains 45% tetrahydrofuran insoluble fraction. Therefore, some studies tried to pre-treat DCLR and remove the tetrahydrofuran-insoluble fraction. The rest part, such as tetrahydrofuran soluble fraction (THFS), could be developed into asphalt modifier. Zhong et al. studied the exaction condition for Shenhua DCLR. The test results presented that optimal conditions were the middle distillate of Shengli coal, 130–150 °C in temperature, 0.5 MPa initial N_2 pressure, 4:1 or 5:1 of the mass ratio of solvent to DCLR and 15–30 min of residence time as well as stirring [15]. Chen et al. extracted THFS from DCLR and studied the properties of THFS modified asphalt binder. The test results indicated that the properties of asphalt binders were best under the conditions of 170 °C mixing temperature and 4% THFS concentration [16].

Most relevant studies focused on the properties of DCLR or THFS modified asphalt binder, but the work on preparation and rheological behaviors of DCLR or THFS modified asphalt binder were limited. There is a need for more research in utilizing DCLR or THFS to develop the standard preparation process and explore the rheological characteristics of asphalt binder. The goal of this study was to optimize the preparation process and investigate the properties, rheological behaviors, sensitivity to temperature and frequency of THFS modified asphalt binder.

2. Objectives and Experimental Scope

The preparation and characterization of THFS modified asphalt binder were investigated in this study. The experimental scope of this study was the following:

- The SK-90 was used as control asphalt binder. Five asphalt binders with different combinations of SK-90 and 0, 4%, 6%, 8%, 10% THFS by weight of SK-90 were prepared.
- The preparation conditions, including shearing temperature, shearing time and shearing rate, were selected and optimized using the orthogonal array test (OATS) and gray correlation analysis (GCA) methods.

- The properties and rheological behaviors of the five asphalt binders were measured according to Penetration performance grade and Superpave performance grade specifications.
- The temperature step test was carried out in Dynamic Shear Rheometer (DSR). The complex modulus index (*GTS*) and stiffness modulus index (*STS*) were regressed using an indication to predict the temperature susceptibility of asphalt binder at high-and-low temperatures, respectively.
- The frequency sweep test in DSR was conducted. The master curves of complex modulus *G** and phase angle *δ* with respect to frequency were plotted and the Christensen-Andersen-Marasteanu (CAM) models, which is a kind of rheological model, were regressed to predict the sensitivity to temperature and frequency.
- The effect of THFS on the rheological behaviors and temperature and frequency susceptibility of asphalt binder was explored through the integrated experimental-computational approach.

3. Test Materials

3.1. Asphalt Binder

The SK-90 asphalt binder used in this study was obtained from South Korea. This binder is widely used in roadway paving construction in China. According to Penetration performance grade and Superpave performance grade specifications, physical properties of SK-90 were measured and satisfied the technical requirement specified by China. The test results are summarized in Table 1.

Table 1. Physical Properties of SK-90.

Items		Specification	SK-90
25 °C Penetration/0.1 mm		80~100	85
Softening Point/°C		≥45	51
10 °C Ductility/cm		≥20	51.8
60 °C Dynamic viscosity/Pa·s		≥160	218
Residue After Rolling Thin Film Oven Test (RTFOT)	Residual penetration ratio/%	≥57	64
	10 °C Residual ductility/cm	≥8	10
Performance Grade (PG)		58–22	

3.2. Tetrahydrofuran Soluble Fraction (THFS)

DCLR was supplied from Inner Mongolia from China Shenhua Coal to Liquid and Chemical Co., Ltd. (Beijing, China). The THFS was obtained from DCLR using Soxhlet extractor and the tetrahydrofuran was used as solvent. The Soxhlet extractor is shown in Figure 1, and the extracting procedures were described as the following:

(1) The DCLR was ground to finer than 2 mm and was sieved using the sieving machine, and then the material passing the 1.18 mm sieve was collected.

(2) DCLR was wrapped in filter paper and placed into the extraction tube of Soxhlet extraction. Thus, the tetrahydrofuran solvent was slowly poured into the extraction tube. The DCLR was soaked in the tetrahydrofuran solvent for 24 h.

(3) The extraction tube was gradually heated to 80 °C. After the temperature reached 80 °C, processing was endured for 24 h.

(4) The THFS solution was collected and further rotated for 30 min at 80 °C with a 400 rpm rate to get THFS.

Figure 1. Soxhlet Extractor. Note: 1: condenser tube; 2: extraction tube; 3: siphon tube; 4: connection tube; 5: extraction flask.

According to Penetration performance grade specifications and four components test procedures, physical properties and four components of THFS were measured, and the test results are listed in Tables 2 and 3.

Table 2. Physical Properties of tetrahydrofuran soluble fraction (THFS).

Items	Specific Gravity/(g/cm^3)	Softening Point/$^\circ$C	25 $^\circ$C Penetration/0.1 mm
Test Results	1.12	140	5

Table 3. Four Components of THFS.

Items	Saturation/%	Aromatic/%	Colloid/%	Asphaltene/%
Test Results	3.8	26.4	14.6	55.2

4. Test and Analysis Methods

4.1. Orthogonal Array Test Strategy (OATS) Method

Orthogonal array test strategy (OATS) enables the test designer to maximize the coverage of the test cases devised for relatively small input domains. OATS is a systematic statistical way to test pair-wise interactions. The testing strategy can be used to reduce the number of test combinations and provide maximum coverage with a minimum number of test cases [17–19]. Some researchers, such as Xu, Sun, et.al, used OATS to prepare rubber or nano-modified asphalt binder and analyze properties affected by the influence factors, including shearing time, preparing temperature and shearing rate. According to OATS analysis results, the optimal scheme of preparation could be determined [20,21]. As a result, in this study, OATS was also applied as a method to determine the optimum preparation process for THFS modified asphalt binder. There were three influence factors (shearing temperature, shearing time and shearing rate) and each of them had three levels. A detailed arrangement of the experiment is shown in Table 4, and the total number of experimental trials was 9 runs.

Table 4. OATS Design.

Runs	A: Shearing Temp./$^\circ$C	B: Shearing Time/min	C: Shearing Rate/rpm	Combinations
1	150	30	2000	$A_1B_1C_1$
2	150	45	4000	$A_1B_2C_2$
3	150	60	6000	$A_1B_3C_3$
4	160	30	4000	$A_2B_1C_2$
5	160	45	6000	$A_2B_2C_3$
6	160	60	2000	$A_2B_3C_1$
7	170	30	6000	$A_3B_1C_3$
8	170	45	2000	$A_3B_2C_1$
9	170	60	4000	$A_3B_3C_2$

4.2. Gray Correlation Analysis (GCA) Method

Gray correlation analysis (GCA) is a relatively new factorial analysis method that can quantitatively assess the degree of correlation among factors in the system dynamics. The GCA method is a combination of quantitative and qualitative analyses. The basic theory of GCA is to determine the degree of correlation between factors based on the degree of similarity in series curves. GCA has the advantage of a small sample size and less calculation and, therefore, is generally used in many areas including natural and social sciences [22,23]. The major steps of GCA are as follows:

(1)　Determination and standardization of reference series and comparative series.

Determine reference series: $X_0 = \{ X_0(k) |\ k = 1, 2, \cdots n \}$

Determine comparative series: $X_i = \{ X_i(k) |\ k = 1, 2, \cdots n \} i = 1, 2, \cdots n$

Standardize reference series: $X_0' = \{ X_0(k) / \overline{X_0} |\ k = 1, 2, \cdots n \}$

Standardize comparative series: $X_i' = \{ X_i(k) / \overline{X_i} |\ k = 1, 2, \cdots n \} i = 1, 2, \cdots n$

(2)　Calculation of the differences: $\Delta_i(k) = |X_0'(k) - X_i'(k)|$

(3)　Calculation of the maximum and minimum differences:

$$M = \max_i \max_k \Delta_i(k); \quad M = \min_i \min_k \Delta_i(k)$$

(4)　Calculation of correlation coefficient:

$$\xi_i(k) = \frac{m + \rho M}{\Delta_i(k) + \rho M}, \quad \rho \in (0, 1) k = 1, 2, \cdots n, \quad i = 1, 2, \cdots n$$

(5)　Calculation of relevancy: $\xi_i = \frac{1}{n} \sum\limits_{k=1}^{n} \xi_i(k), \quad i = 1, 2, \cdots n$

(6)　Ranking of the calculated relevancies: the larger the relevancy ξ_i, the higher the degree of correlation between comparative series X_i and reference series X_0.

(7)　Calculation of correlation degree (Y):

$$Y_i = \sum\limits_{k=1}^{5} b_{ij} \times (\text{test result of each index}), \quad i = 1, 2, \cdots 9$$

$$b_{ij} = \frac{\text{the proportion of each index}}{\text{the difference between max and min valus of each index}}, \quad j = 1, 2, 3, 4, 5$$

4.3. Penetration Performance Grade Tests

The physical properties of asphalt binder by applying Penetration performance grade tests included 25 °C penetration according to ASTM D5 [24], 10 °C ductility according to ASTM D113 [25], softening point according to ASTM D36 [26], and 135 °C rotational viscosity (RV) using the Brookfield viscometer according to ASTM D4402 [27].

4.4. Dynamic Shear Rheometer (DSR) Test

Samples were prepared for unaged asphalt binder with a 1 mm thickness and 25 mm diameter. For PAV aged asphalt binder, samples were fabricated with a 2 mm thickness and 8 mm diameter. According to the AASHTO T 315 [28], the temperature step test was conducted on the unaged asphalt binder samples, the temperature ranged from 46 °C to 76 °C with a 6 °C increment performed at a fixed frequency of 10 rad/sec at a controlled stress mode of 120 Pa. Moreover, the temperature step test was also performed for the PAV asphalt binder samples; the temperature varied from 19 °C to 31 °C with a 3 °C increment which ran at a fixed frequency of 10 rad/sec at a controlled stress mode of 120 Pa.

The frequency sweep test was performed at 30 °C, 45 °C and 60 °C for the unaged asphalt binder sample using a 25 mm diameter spindle and a gap of 1 mm. The frequency varied from 0.01 Hz to 10 Hz and ran at 1% in controlled stress mode. In addition, the test parameters, such as phase

angle δ, complex shear modulus G^*, rutting parameter $G^*/sin\delta$, and fatigue parameter $G^*·sin\delta$, could be obtained. Therefore, a minimum value of $G^*/sin\delta$ to assign the high-temperature grade should be 1.0 for unaged asphalt binder and 2.2 for RTFO-aged asphalt binder. A maximum value of $G^*·sin\delta$ should be 5000 for PAV-aged asphalt binder as per the Superpave performance grade specification.

4.5. Bending Beam Rheometer (BBR) Test

The BBR test was conducted on PAV aged asphalt binder samples according to AASHTO T313 [29]. The test temperatures were −6 °C, −12 °C and −18 °C limited to 240 s under a constant load of 1000 mN. The test parameters, such as creep stiffness S and m-value, were obtained. Therefore, the minimum m-value should be 0.3 and the maximum S should be 300 MPa for determining the low-temperature grade of asphalt binder as per the Superpave performance grade specification.

5. Results and Discussions

5.1. OATS Analysis Results

Figure 2 and Table 5 list the OATS analysis results.

The test results were evaluated by the extreme difference analysis method to optimize the preparation process. According to Table 5, the ranking of influence factor impacting 25 °C penetration, 10 °C ductility, softening point and 135 °C RV was shearing time, followed by shearing temperature and shearing rate, and the optimal combination was suggested to be $A_2B_2C_2$.
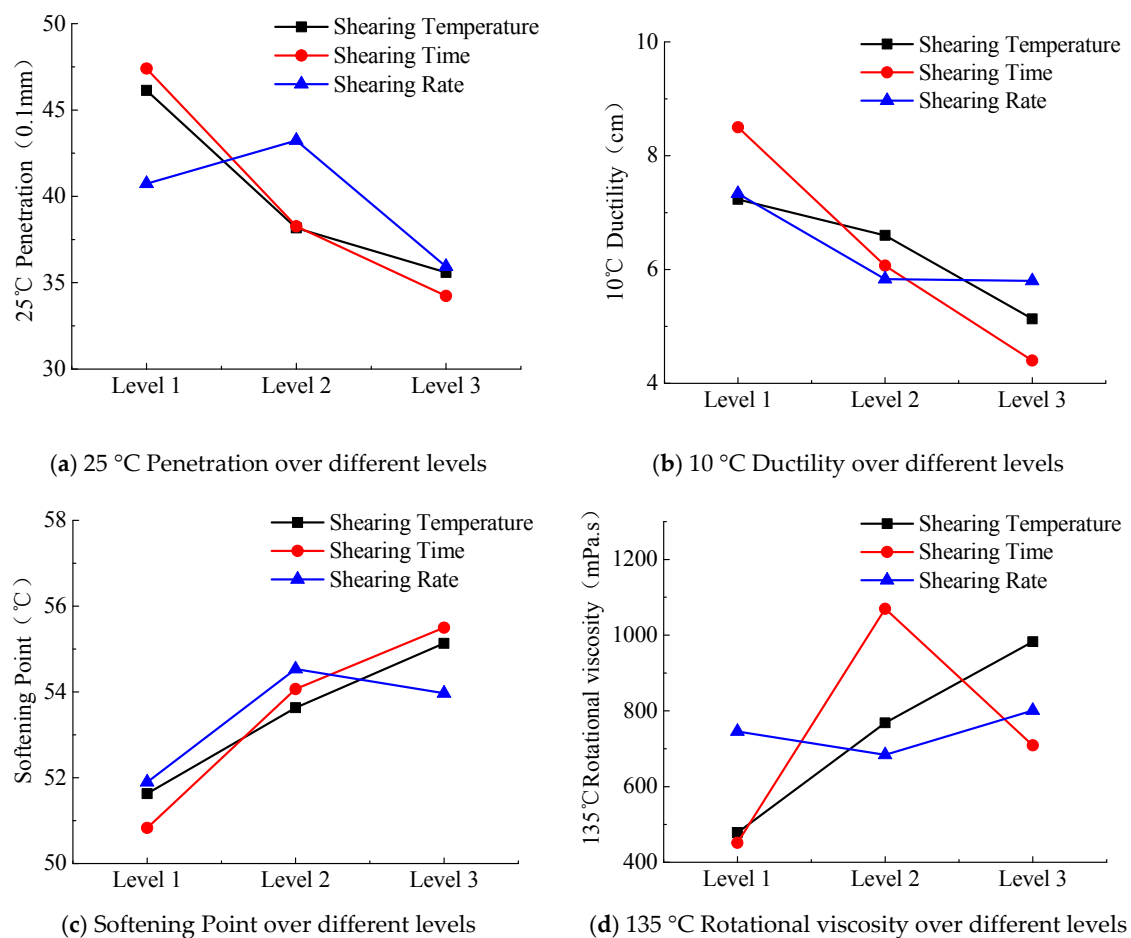

(**a**) 25 °C Penetration over different levels

(**b**) 10 °C Ductility over different levels

(**c**) Softening Point over different levels

(**d**) 135 °C Rotational viscosity over different levels

Figure 2. Average Value Change of Five Indicators over Influence Factors and their Levels.

Table 5. OATS Analysis Results.

Items		A: Shearing Temperature/°C	B: Shearing Time/min	C: Shearing Rate/rpm
25 °C Penetration	Range	10.533	13.167	7.300
	Optimal combination		$A_2B_2C_3$	
10 °C Ductility	Range	2.100	4.100	1.533
	Optimal combination		$A_1B_1C_1$	
Softening Point	Range	3.500	4.667	2.633
	Optimal combination		$A_2B_2C_2$	
135 °C RV	Range	504.300	618.367	117.467
	Optimal combination		$A_1B_2C_2$	

5.2. GCA Analysis Results

The GCA analysis results are shown in Table 6.

Table 6. GCA Analysis Results.

Combinations	25 °C Penetration	10 °C Ductility	Softening Point	135 °C RV	Correlation Degree
$A_1B_1C_1$	0.5954	0.7376	0.5650	0.5826	216.4496
$A_1B_2C_2$	0.5933	0.7407	0.5747	0.6091	217.5866
$A_1B_3C_3$	0.5214	0.9914	0.9013	1.0000	195.1453
$A_2B_1C_2$	0.8856	0.8031	0.6705	0.6056	214.3054
$A_2B_2C_3$	0.4562	1.0000	0.6607	0.4480	216.9869
$A_2B_3C_1$	0.7361	0.7085	1.0000	0.9417	201.9705
$A_3B_1C_3$	0.5765	0.8313	0.8609	0.7440	209.6878
$A_3B_2C_1$	1.0000	0.9001	0.9443	0.5146	216.9994
$A_3B_3C_2$	0.3535	0.4493	0.4501	0.4980	207.4202
Correlation	0.6353	0.7958	0.7364	0.6604	-
Factor ratio/%	22.467	28.140	26.039	23.352	-

The test results in Table 6 addressed that the combination $A_1B_2C_2$ had the highest correlation degree, which presented that the physical properties of this asphalt binder were the best compared to the other test samples. As a result, the following optimal combination was recommended: $A_1B_2C_2$.

5.3. Optimal Preparation Process

The physical properties of THFS modified asphalt binder with different combinations ($A_2B_2C_2/A_1B_2C_2$) recommended using OATS and GCA analysis results were different and further compared. The test results are shown in Table 7.

Table 7. Physical properties of Asphalt Binders with Different Combinations.

Combinations	25 °C Penetration/0.1 mm	10 °C Ductility/cm	Softening Point/°C	135 °C RV/mPa·s	Methods
$A_2B_2C_2$	49.6	9.1	50.1	527.4	OATS
$A_1B_2C_2$	51.8	9.7	52.1	531.6	GCA

It could be reported that the physical properties of asphalt binder prepared according the GCA analysis result ($A_1B_2C_2$) was better than that fabricated according the OATS analysis result ($A_2B_2C_2$). The optimal combination for preparation process acquired in this study was a shearing temperature of 150 °C, shearing time of 45 min and shearing rate of 4000 rpm. Consequently, the following steps schematically summarized for THFS modified asphalt binder preparation procedure:

(1) The SK-90 and THFS were heated in a 120 °C and 150 °C oven respectively until they melted and were poured in a container.

(2) The 4%, 6%, 8%, and 10% THFS by weight of the SK-90 were added gradually around 1 g/min to SK-90.

(3) After THFS was added to SK-90, the blending material was sheared for 45 min at the speed of 4000 rpm while maintaining a temperature of 150 °C to ensure that THFS was homogenously mixed and well dispersed inside the medium of SK-90.

5.4. Physical Properties of THFS Modified Asphalt Binder

Physical properties of asphalt binders with different THFS contents were measured, and are listed in Table 8.

Table 8. Physical properties of Asphalt Binders with Different THFS Contents.

	Items	0% THFS	4% THFS	6% THFS	8% THFS	10% THFS
	25 °C Penetration/0.1 mm	85.0	58.7	56.8	54.0	49.6
	Softening Point/°C	51.0	48.2	49.0	49.4	50.1
	10 °C Ductility/cm	51.8	11.3	10.2	9.9	9.7
	135 °C RV/mPa·s	365.8	465.7	567.7	582.3	627.4
Residue After RTFOT	Residual penetration ratio/%	64.0	53.2	51.3	47.9	46.5
	10 °C Residual ductility/cm	10.0	4.3	3.8	3.6	3.2
	Performance Grade (PG)	58–22	64–22	64–22	64–16	64–16

The test results indicated that there was a remarkable improvement in 135 °C RV, softening point and decrement in 25 °C penetration of THFS modified asphalt binders compared to SK-90. It could be demonstrated that the high-temperature properties of asphalt binder improved due to the addition of THFS and increased as THFS content increased. However, the test results in Table 8 also mentioned that there was a remarkable reduction in 10 °C ductility of THFS modified asphalt binder compared to SK-90, which indicated that the low-temperature properties of asphalt binder decreased after adding THFS. Furthermore, when THFS content was higher than 6%, the 10 °C ductility of asphalt binder failed to meet the technical requirement specified by China ($\geq$10 cm). A possible explanation for this tendency was THFS with higher asphaltene content reduced the flexibility of asphalt binder at low temperatures but improved the stiffness and hardness of asphalt binder at high temperatures. The movement of asphalt binder molecular chains might be limited by the layers of THFS at high temperatures during formation of an exfoliated structure, which led to an increase in softening point and RV, but the penetration and ductility decreased.

Therefore, it could be noticed from Table 8 that asphalt binders with different THFS contents had a slight decrease in residual penetration ratio and residual ductility values after being subjected to RTFO aging. This decrease was statistically insignificant at the 5% significance level (95% confidence interval), which addressed that aging had a little effect on the properties of THFS modified asphalt binder.

Compared with SK-90, as THFS content increased, the high-temperature PG value of the asphalt binder increased from 58 °C to 64 °C, but the low-temperature PG value decreased from −22 °C to −16 °C. This indicated that there was an interaction of THFS with asphalt binder that would affect not just high-temperature properties of asphalt binder, but also low-temperature properties. The optimum THFS content should be recommended while considering a balance between the high-and-low temperature properties of asphalt binder. In this study, the optimum THFS content was recommended to be 6%.

5.5. Temperature Susceptibility of THFS Modified Asphalt Binder

5.5.1. Resistance to Rutting at High Temperature

Figure 3 illustrates the *G**/*sinδ* values of asphalt binders versus test temperatures.
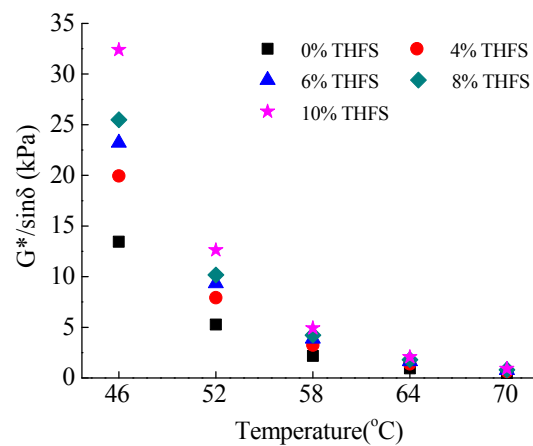
Figure 3. *G**/*sinδ* Values of Asphalt Binders over Temperatures.

According to the test results in Figure 3, the *G**/*sinδ* values of asphalt binders decreased across the test temperature ranges(46 °C to 76 °C with a 6 °C increment). Under the identical condition of THFS content, there was a major decrease in *G**/*sinδ* value at low temperatures, but a minor decrease was observed at high temperatures. Moreover, the *G**/*sinδ* had a good exponential correlation with the test temperature with a high correlation coefficient R^2 ranging from 0.9981 to 0.9989 and is given in Equation (1)

$$G*/sin\delta = A \cdot e^{B \cdot T} \tag{1}$$

where: *G**/*sinδ* is the rutting parameter of asphalt binder, kPa;

T is the temperature, °C;

A and *B* are the regression coefficients.

When taking the logarithm of Equation (1), there was a good linear relationship between *lg (G*/sinδ)* and test temperature *T* and is shown in Equations (2) and (3).

$$lg(G*/sin\delta) = GTS \cdot T + C \tag{2}$$

$$GTS = \frac{lg(G^* / \sin \delta_1) - lg(G^* / \sin \delta_2)}{T_1 - T_2} \tag{3}$$

GTS is the slope of *lg (G*/sinδ)* with respect to the test temperature *T*, which can be used to characterize the temperature susceptibility of asphalt binder at high temperatures. A higher absolute *GTS* value indicates that asphalt binder is more sensitive to high temperatures. The *GTS* values of asphalt binders are listed in Figure 4.

From the test results in Figure 4, it could be observed that the absolute *GTS* values of THFS modified asphalt binders were lower than that of SK-90 and decreased with the increase in THFS content. It showed that the addition of THFS resulted in decreased temperature susceptibility of asphalt binder. The asphalt binder with higher THFS content was less sensitive to temperature. However, for THFS modified asphalt binders, the *G**/*sinδ* values were higher than that of SK-90 under identical conditions of temperature and increased gradually as THFS content increased. This observation could be attributed to THFS had a higher asphaltene content, resulting in asphalt binder with a higher RV, greater stiffness, and hardness compared to SK-90, which improved the resistance to permanent deformation.
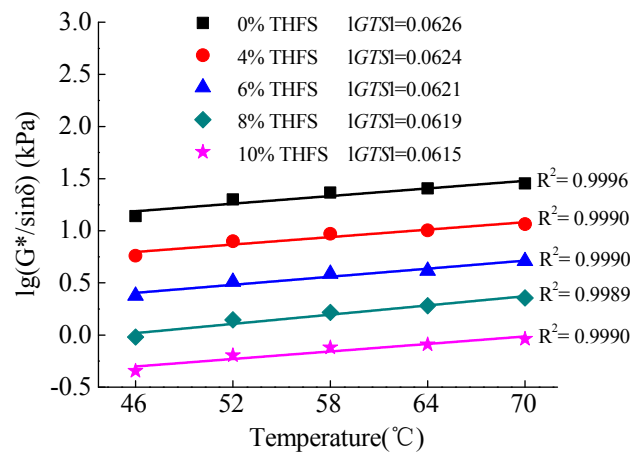
Figure 4. Relationships between *lg*(*G*/sinδ*) of Asphalt Binder and Temperature.

5.5.2. Resistance to Fatigue at Intermediate Temperature

Figure 5 represents the *G*·sinδ* values of asphalt binders versus test temperatures.

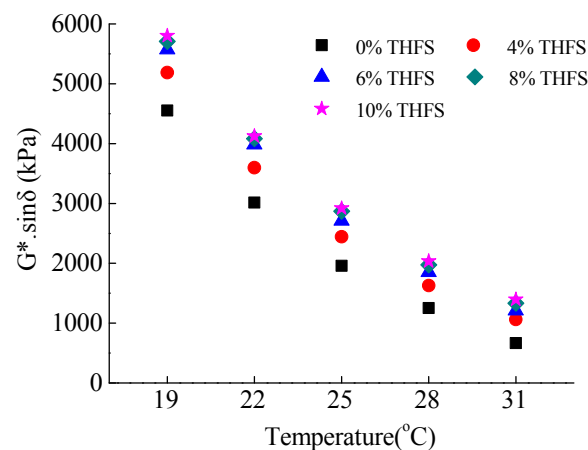**Figure 5.** *G*·sinδ* Values of Asphalt Binders over Temperatures.

From the test results in Figure 5, it could be observed the *G*·sinδ* values of asphalt binders decreased across the test temperature ranges. The decrease in *G*·sinδ* value was nearly identical in the range of test temperature from 19 °C to 31 °C. Moreover, the *G*·sinδ* had a good linear correlation with test temperature with a high correlation coefficient R^2 ranging from 0.9981 to 0.9989. This phenomenon could be explained by the addition of THFS, which reduced the potential for fatigue cracking at intermediate temperatures due to lower malthene and higher asphaltene contents. Subsequently, for THFS modified asphalt binders, the *G*·sinδ* values were higher than that of SK-90 under identical conditions of test temperature and increased as THFS content increased.

5.5.3. Resistance to Thermal Cracking at Low Temperature

Figure 6 reports the *S* values of asphalt binders over test temperatures.

Figure 6 demonstrates that the *S* values of asphalt binders increased, compared to SK-90 under an identical test temperature. It showed that THFS modified asphalt binder was more prone to thermal cracking at low temperatures compared to SK-90. A possible explanation for this tendency was THFS with a higher asphaltene and lower malthene content reduced the flexibility and elasticity of asphalt binder at low temperatures.
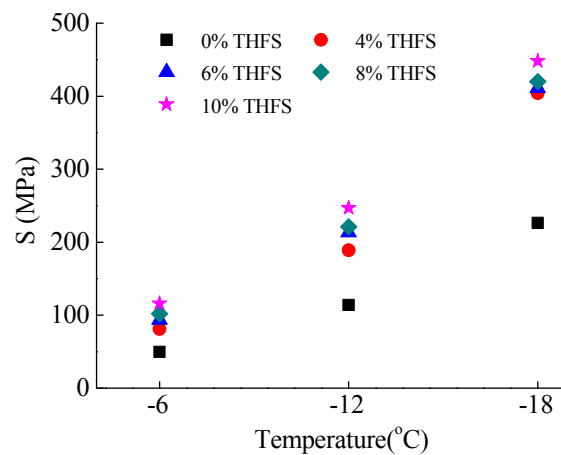
Figure 6. *S* Values of Asphalt Binders over Temperatures.

Under the identical conditions of THFS content, the *S* values of asphalt binders decreased as the test temperature increased and had a good linear correlation with temperature with a high correlation coefficient R^2 ranging from 0.9646 to 0.9853. If taking the logarithm of *S* and temperature *T*, it was found that the *lg(S)* had a good linear correlation with test temperature, and is given as Equations (4) and (5).

$$lg(S) = STS \cdot T + C \tag{4}$$

$$STS = \frac{lg(S_1) - lg(S_2)}{T_1 - T_2} \tag{5}$$

in which: *S* is creep stiffness (MPa);

T is the test temperature (°C);

C is the regression coefficient;

STS is the slope of *lg (S)* to the test temperature.

The *STS* is the slope of *lg (S)* to the test temperature and is followed in Equation (5), which can be used to detect the temperature susceptibility of asphalt binder at low temperatures. A higher absolute *STS* value indicates that asphalt binder is more sensitive to thermal cracking at low temperatures. The *STS* values of asphalt binders are listed in Figure 7.
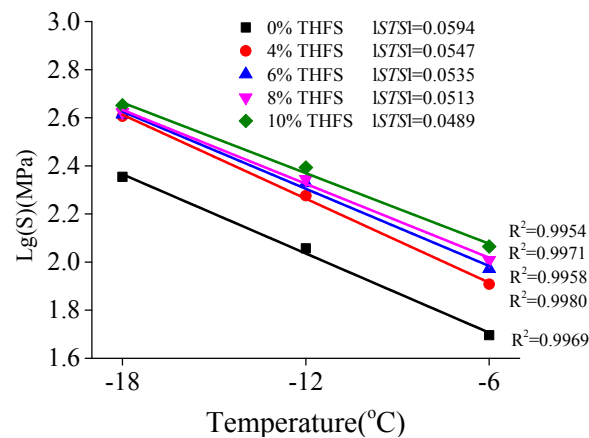

Figure 7. Relationships between *lg(S)* of Asphalt Binders and Temperatures.

According to the test results in Figure 7, it could be found that the absolute *STS* values of asphalt binders were lower than that of SK-90 and 10% THFS modified asphalt binder had the lowest absolute

STS value. It showed that the addition of THFS resulted in a decrease in the temperature susceptibility of asphalt binder at low temperatures. The asphalt binder with a higher THFS content was less sensitive to thermal cracking at low temperatures.

5.5.4. Frequency Susceptibility of the THFS Modified Asphalt Binder

On the basis of time-temperature equivalence principle and through curve fitting using Sigmoidal function, the G^* and δ master curves of asphalt binders with respect to frequencies ranging from 0.01 Hz to 50 Hz were regressed. The G^* and δ master curves are plotted in Figure 8.
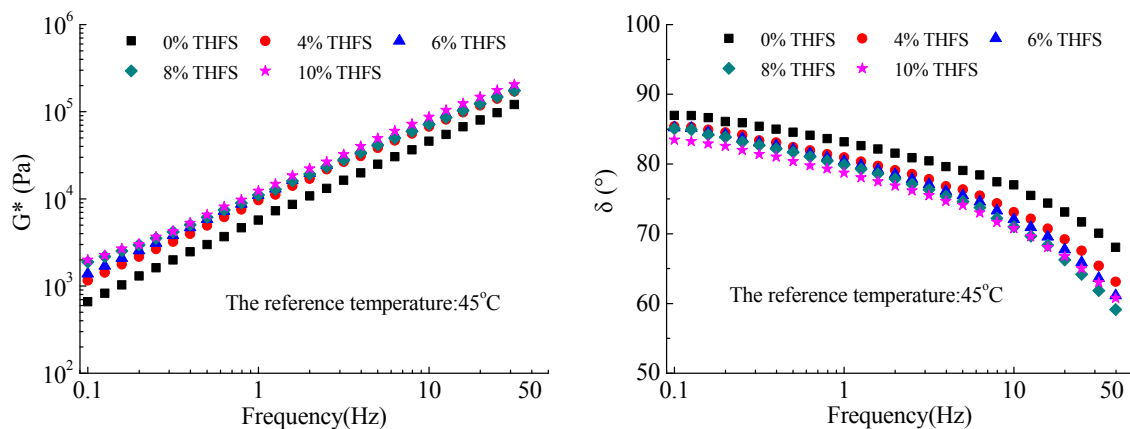

Figure 8. G^* and δ Master Curves of Unaged Asphalt Binders over Frequencies.

There was a similar increase in G^* value and decrease in δ value for asphalt binders across frequencies ranging from 0.01 Hz to 50 Hz. This could be because the pavement response and deformation were instantaneous and small caused by a higher frequency, which indicates a shorter loading time. The increase in G^* values and decrease in δ values resulted in an improved frequency and exhibited elastic behavior during shorter loading times because asphalt binder would recover from some deformations due to elastic stored energy. Under identical frequencies, the G^* values of THFS modified asphalt binders were higher than that of SK-90, but the δ values were lower than that of SK-90, which indicated that at a constant frequency, the addition of THFS could improve the stiffness and elastic characteristics as well as the potential resistance to permanent deformation.

Moreover, for THFS modified asphalt binder, there was a slight increment in G^* values and a minor reduction in δ values as THFS content increased at the same frequency. This can be attributed to the interaction of THFS and asphalt binder that form more and more large molecules and limit the movement of molecular chains of asphalt binder. The increase in G^* values and decrease in δ values were statistically significant at the 5% significance level, which indicated that THFS content had a significant effect on the frequency susceptibility of THFS modified asphalt binder.

5.5.5. Frequency susceptibility based on CAM model

The Christensen-Andersen-Marasteanu (CAM) model is a kind of rheological model adding a parameter, m_e, on the basis of basic shape parameters of the CA model [30–33]. Most rheological models are mainly focused on researching the rheological properties of asphalt, however, the CAM model can not only describe the rheological properties of asphalt but also analyze the rheological properties of mixtures. The CAM model includes four equations: the complex modulus master curve equation, the storage modulus master curve equation, the phase angle equation and temperature shift factor equation. These equations characterize the proportion of viscosity and elasticity of asphalt, and

also exhibit the temperature sensitivity of viscoelastic properties of asphalt. The equation of the CAM model is shown in Equation (6)

$$G^* = G_e^* + \frac{G_g^* - G_e^*}{\left[1 + (f_c/f')^k\right]^{m_e/k}} \tag{6}$$

where: G_e^* is the equilibrium complex modulus of asphalt (kPa). It is G^* when frequency reaches zero or the temperature is very high;

G_g^* is the glassy complex modulus (kPa). It is G^* when frequency reaches infinity or the temperature is very low;

f_c is the elastic limit threshold (Hz);

f' is the reduced frequency, related to temperature and strain (Hz);

k and m_e are shape parameters, without sizes.

The zones beyond the threshold frequency are the low-frequency stable zone and high-frequency stable zone. Correspondingly, it is called equilibrium complex modulus G_e^* and glassy complex modulus G_g^*. The breakpoint is called the low-frequency break point when the low-frequency stable zone changes into the rheological zone. The break point symbolizes the change in physical form of asphalt. The intercept between G_g^* (f_c) and G_g^* is recorded as R, which is related to shape parameters k and m_e. R refers to the width of the relaxation spectrum. A larger value of R indicates that it is easy to change from elastic to viscous behaviors. It also indicates less sensitivity to frequency changes. The parameter R is shown in Equation (7).

$$R = lg\frac{2^{m_e/k}}{1 + (2^{m_e/k} - 1)G_e^*/G_g^*} \tag{7}$$

Since $G_e^* = 0$ for asphalt binder, the equation of R is as follows (8):

$$R = \frac{m_e}{k}lg2 \tag{8}$$

Table 9 lists the fitting parameters of asphalt binders based on the CAM model.

Table 9. The fitting parameters based on the CAM model.

Asphalt Binders	G_g^*/kPa	f_c/Hz	m_e	k	R_G	R^2
SK-90	2.63×10^5	81.680	0.843	3.808	0.067	0.9996
4% THFS + SK-90	3.31×10^5	67.836	0.833	3.328	0.075	0.9996
6% THFS + SK-90	3.57×10^5	66.571	0.813	2.998	0.082	0.9999
8% THFS + SK-90	3.88×10^5	64.537	0.809	2.549	0.096	0.9990
10% THFS + SK-90	3.91×10^5	58.783	0.806	2.481	0.098	0.9994

The test results in Table 9 presented that the correlation coefficients R^2 were higher than 0.9990, very close to 1, which indicated that the CAM model was very reliable in predicting the rheological behavior and frequency susceptibility of asphalt binder. In the CAM model, the G_g^* values of asphalt binders were higher than that of SK-90, and 10% THFS modified asphalt binder had the highest G_g^* value. It showed that THFS modified asphalt binder had more resistance to permanent deformation at frequencies ranging from 0.1 Hz to 50 Hz. Subsequently, asphalt binder with higher f_c value indicates it had a good resistance to thermal cracking at low temperatures. Compared with SK-90, the f_c value of THFS modified asphalt binder decreased and 10% THFS modified asphalt binder had the lowest f_c value. It could be predicted that THFS modified asphalt binder was more prone to thermal cracking at low temperatures. This remark was similar to the BBR test results.

Furthermore, asphalt binder with a higher R_G value represented that the ratio of elastic to viscous was high and less sensitive to frequency. According to the test results in Table 9, it could be observed that 10% THFS modified asphalt binder had the highest R_G and lowest m_e, and k, which indicated that 10% THFS modified asphalt binder had a wider relaxation spectrum and less sensitivity to frequency. It also could be predicted that THFS modified asphalt binder had a better temperature and frequency susceptibility compared to SK-90. In other words, the addition of THFS could decrease the temperature and frequency susceptibility of asphalt binder.

6. Conclusions

Based upon the analysis and results of this study, basic conclusions can be drawn:

- The optimal preparation process, such as 150 °C shearing temperature, 45 min shearing time and 4000 rpm shearing rate, was determined on the basis of OATS and GCA analysis results.
- The high-temperature properties of asphalt binder were improved, the low-temperature properties and resistance to fatigue decreased due to the addition of THFS and the increase in THFS content. The 4~6% THFS content achieved a balance in the high-and-low temperature properties of asphalt binder.
- Based on the temperature step test results, the *GTS* and *STS* were regressed as indicators to predict the temperature susceptibility of asphalt binder. The absolute *GTS* and *STS* values decreased with the increase in THFS content, which showed a reduction in temperature susceptibility of asphalt binder due to the addition of THFS.
- The CAM model for asphalt binder with high correlation coefficients R^2 ranged from 0.9990 to 0.9999, very close to 1, which indicated that the CAM model was very reliable in predicting the rheological behavior and frequency susceptibility of asphalt binder. On the basis of parameters, such as $G_g{}^*$, R_G, f_c, m_e and k, variation tendency, THFS modified asphalt binder had more resistance to rutting but less sensitivity to temperature and frequency.

Author Contributions: Jie Ji and Hui Yao made substantial contributions to the conception, design and analysis of the whole paper; Wenhua Zheng, Hao Wu and Yuefeng Shi performed the experiments; Zhi Suo and Ying Xu analyzed the data; Zhanping You revised the paper.

Conflicts of Interest: The authors declare that they have no conflict of interest.

References

1. Mochida, I.; Okuma, O.; Yoon, S.H. Chemicals from direct coal liquefaction. *Chem. Rev.* **2014**, *114*, 1637–1672. [CrossRef] [PubMed]
2. Schulz, H. Short history and present trends of Fischer–Tropsch synthesis. *Appl. Catal. A Gen.* **1999**, *186*, 3–12. [CrossRef]
3. Hildebrandt, D.; Glasser, D.; Hausberger, B.; Patel, B.; Glasser, B.J. Producing transportation fuels with less work. *Science* **2009**, *323*, 1680–1681. [CrossRef] [PubMed]
4. Weirauch, W. HPImpact: Benefits of coal liquefaction technology. *Hydrocarb. Process.* **2007**. Available online: https://www.researchgate.net/publication/293392610_HPImpact_Benefits_of_coal_liquefaction_technology (accessed on 9 November 2017).
5. Ji, J.; Wang, D.; Shi, Y.F.; Xu, S.F.; Suo, Z. Study on the Performances of the DCLR Modified Asphalt Mixtures. *J. Zhengzhou Univ. Eng. Sci.* **2016**, *37*, 67–71.
6. Khare, S.; Dell'Amico, M. An overview of solid–liquid separation of residues from coal liquefaction processes. *Can. J. Chem. Eng.* **2013**, *91*, 324–331. [CrossRef]
7. Wang, J.L.; Yao, H.W.; Nie, Y.; Bai, L.; Zhang, X.P.; Li, J.W. Application of iron-containing magnetic ionic liquids in extraction process of coal direct liquefaction residues. *Ind. Eng. Chem. Res.* **2012**, *51*, 3776–3782. [CrossRef]

8. Behnood, A.; Olek, J. Rheological properties of asphalt binders modified with styrene-butadiene-styrene (SBS), ground tire rubber (GTR), or polyphosphoric acid (PPA). *Constr. Build. Mater.* **2017**, *151*, 464–478. [CrossRef]

9. Kök, B.V.; Çolak, H. Laboratory comparison of the crumb-rubber and SBS modified bitumen and hot mix asphalt. *Constr. Build. Mater.* **2011**, *25*, 3204–3212. [CrossRef]

10. Kök, B.V.; Yilmaz, M.; Geçkil, A. Evaluation of Low-Temperature and Elastic Properties of Crumb Rubber- and SBS-Modified Bitumen and Mixtures. *J. Mater. Civ. Eng.* **2013**, *25*, 257–265. [CrossRef]

11. Lv, D.M.; Wei, Y.C.; Bai, Z.Q.; Bai, J.; Kong, L.X.; Guo, Z.X.; Yan, J.C.; Li, W. An approach for utilization of direct coal liquefaction residue: Blending with low-rank coal to prepare slurries for gasification. *Fuel* **2015**, *145*, 143–150. [CrossRef]

12. Nan, X.; Zhou, Y.; Qiu, J.S.; Wang, Z.H. Preparation of carbon nanofibers/carbon foam monolithic composite from coal liquefaction residue. *Fuel* **2010**, *89*, 1169–1171.

13. Ji, J.; Shi, Y.F.; Suo, Z.; Xu, S.F. Properties and Micro-structure of DCLR blending modified asphalt. *J. Beijing Univ. Technol.* **2015**, *41*, 1049–1053.

14. Zhang, D.R.; Luo, R.; Chen, Y.; Sheng, Y. Performance Analysis of DCLR-modified Asphalt Based on Surface Free Energy. *China J. Highw. Transp.* **2016**, *29*, 22–28.

15. Zhong, J.L.; Li, W.B.; Shi, S.D.; Zhu, X.S. Solvent extraction research on organic matter in direct coal liquefaction residue. *J. China Coal Soc.* **2012**, *37*, 316–322.

16. Chen, J.; Sun, M.; Dai, X.M.; Yao, Y.; Liu, Y.Y.; He, M.; Lü, B.; Zhao, X.L.; Ma, X.X. Asphalt modification with direct coal liquefaction residue based on benzaldehyde crosslinking agent. *J. Fuel Chem. Technol.* **2015**, *43*, 1052–1060.

17. Cui, W.G.; Li, X.H.; Zhou, S.B.; Weng, J. Investigation on process parameters of electrospinning system through orthogonal experimental design. *J. Appl. Polym. Sci.* **2007**, *103*, 3105–3112. [CrossRef]

18. Hong, H.C.; Huang, H.W.; Bai, Y.J. Optimization of Intake and Exhaust System for FSAE Car Based on Orthogonal Array Testing. *Int. J. Eng. Technol.* **2012**, *2*, 1–5.

19. Tsoi, W.Y.I.; Kan, C.W.; Yuen, C.W.M. Using ageing effect for hydrophobic modification of cotton fabric with atmospheric pressure plasma. *BioResources* **2011**, *6*, 3424–3439.

20. Xu, A.H.; Wang, X.W.; Xiong, R.; Chen, H.X.; Fang, J.H.; Kuang, D.L.; Wang, X.L.; Liu, Z.M. Experimental Investigation on Preparation Technology and Performance of Rubber Powder Modified Asphalt. *Bull. Chin. Ceram. Soc.* **2017**, *36*, 1326–1344.

21. Sun, L.; Zhu, H.R.; Xin, X.T.; Wang, H.Y.; Gu, W.J. Preparation of Nano-Modified Asphalt and Its Road Performance Evaluation. *China J. Highw. Transp.* **2013**, *26*, 15–22.

22. Kuo, Y.; Yang, T.; Huang, G.W. The use of grey relational analysis in solving multiple attribute decision-making problems. *Comput. Ind. Eng.* **2008**, *55*, 80–93. [CrossRef]

23. Gao, Y.F.; Wang, J.; He, Z.D. Gray Correlation Analysis on Influence Factors of Postgraduates' Innovative Capacity. *J. Theor. Appl. Inf. Technol.* **2013**, *49*, 1–10.

24. ASTM. *Standard Test Method for Penetration of Bituminous Materials*; ASTM D5; ASTM: West Conshohocken, PA, USA, 2005.

25. ASTM. *Standard Test Method for Ductility of Bituminous Materials*; ASTM D113; ASTM: West Conshohocken, PA, USA, 2007.

26. ASTM. *Standard Test Method for Softening Point of Bitumen (Ring-and-Ball Apparatus)*; ASTM D36; ASTM: West Conshohocken, PA, USA, 2014.

27. ASTM. *Standard Test Method for Viscosity Determination of Asphalt at Elevated Temperatures Using a Rotational Viscometer*; ASTM D4402; ASTM: West Conshohocken, PA, USA, 2006.

28. AASHTO. *Standard Test Method for Determining the Rheological Properties of Asphalt Binder Using a Dynamic Shear Rheometer (DSR)*; AASHTO T 315; AASHTO: West Conshohocken, PA, USA, 2008.

29. AASHTO. *Standard Test Method for Determining the Flexural Creep Stiffness of Asphalt Binder Using the Bending Beam Rheometer (BBR)*; AASHTO T 313; AASHTO: West Conshohocken, PA, USA, 2008.

30. Bahia, H.; Hanson, D.; Zeng, M.; Zhai, H.; Khatri, M.A.; Anderson, R.M. *A Project NCHRP 9–10 Superpave Protocols for Modified Asphalt Binders*; Draft Topical Report (Task 9), Prepared for National Cooperative Highway Research Program; Transportation Research Board; National Research Council: West Conshohocken, PA, USA, 2000.

31. Chailleux, E.; Ramond, G.; Such, C.; de la Roche, C. A mathematical-based master-curve construction method applied to complex modulus of bituminous materials. *Road Mater. Pavement Des.* **2006**, *7* (Suppl. 1), 75–92. [CrossRef]

32. Chambrion, P.; Bertau, R.; Ehrburger, P. Effect of polar components on the physico-chemical properties of coal tar. *Fuel* **1995**, *74*, 1284–1290. [CrossRef]

33. Zeng, M.; Bahia, H.U.; Zhai, H.; Anderson, M.R.; Turner, P. Rheological modeling of modified asphalt binders and mixtures (with discussion). *J. Assoc. Asph. Paving Technol.* **2001**, *70*, 403–441.